Spatially Resolved Characterization of Cellulose Nanocrystal–Polypropylene Composite by Confocal Raman Microscopy

Umesh P. Agarwal,* Ronald Sabo, Richard S. Reiner, Craig M. Clemons, Alan W. Rudie

USDA FS, Forest Products Laboratory, Madison, WI 53726 USA

Raman spectroscopy was used to analyze cellulose nanocrystal (CNC) –polypropylene (PP) composites and to investigate the spatial distribution of CNCs in extruded composite filaments. Three composites were made from two forms of nanocellulose (CNCs from wood pulp and the nanoscale fraction of microcrystalline cellulose) and two of the three composites investigated used maleated PP as a coupling agent. Raman maps, based on cellulose and PP bands at 1098 and 1460 cm^{-1}, respectively, obtained at 1 μm spatial resolution showed that the CNCs were aggregated to various degrees in the PP matrix. Of the three composites analyzed, two showed clear existence of phase-separated regions: Raman images with strong PP and absent/weak cellulose or vice versa. For the third composite, the situation was slightly improved but a clear transition interface between the PP-abundant and CNC-abundant regions was observed, indicating that the CNC remained poorly dispersed. The spectroscopic approach to investigating spatial distribution of the composite components was helpful in evaluating CNC dispersion in the composite at the microscopic level, which helped explain the relatively modest reinforcement of PP by the CNCs.

Index Headings: **Raman mapping; Confocal Raman microscopy; Nanocrystalline cellulose; Polypropylene; Composite.**

INTRODUCTION

There is growing interest in making composites that are based on renewable materials.[1,2] Because such composites are biodegradable and environmentally friendly, they are desirable replacements for conventional composites based on petroleum feedstock. One such category of materials composed of wood fiber/flour and plastics is wood plastic composites.[3–5] In these materials, wood fiber is used as an inexpensive component along with a thermoplastics matrix such as polyethylene (PE), polypropylene (PP), and polyvinyl chloride (PVC). Another approach to making green composites has been to use cellulose from a variety of sources: higher plants, algae, bacteria, and tunicates.[6–8] In particular, bacterial cellulose has been shown to be capable of mechanical reinforcement of both thermoplastic and thermoset resins for making composites.[9,10] Cellulose nanocrystals (CNCs) are such a material that is mechanically strong and nano-dimensional and have the advantage of being conveniently produced from naturally abundant cellulose fibers. CNCs are the rod-shaped nano-size crystalline regions that are contained within cellulose microfibrils and are isolated when native cellulose is subjected to strong acid hydrolysis.[11,12] The dimensions of the CNCs vary depending upon the source of cellulose and range from 3 to 20 nm in diameter and 100 to 1000 nm in length.[8,12,13] The Young's modulus of CNC has been reported to range from 138 to 167 GPa.[8,13,14]

Received 15 December 2011; accepted 22 March 2012.
* Author to whom correspondence should be sent. E-mail: uagarwal@fs.fed.us.
DOI: 10.1366/11-06563

The CNCs can be incorporated as the load-bearing component in composites to enhance the properties of synthetic and other polymer matrices. This will give rise to composites with improved strength. Obtaining information on composition and structure of the CNC composite is essential for correlating structure to mechanical properties. Research investigations are needed to understand the physicochemical aspects of the CNCs, the polymer matrix, and their interactions. This is extremely valuable because such findings will allow new experimental strategies for optimizing composite processing and production. In the present investigation, composites of PP containing 2 wt. % CNC were investigated. A low concentration of CNC was considered desirable from the view points of efficient reinforcement at low cost.

Although a number of techniques were used in the CNC-PP composite characterization, this report focuses on analysis using Raman spectroscopy. The technique requires no sample preparation and provides structural information that is sensitive to intra- and inter-molecular interactions. Confocal Raman microscopy[15] was selected for detailed analysis at the microscopic level because it provides chemically specific information at high spatial resolution. Compared to electron microscopy, which has much higher resolution but poor contrast between CNCs and PP, Raman microscopy easily discriminates between these. Raman mapping cannot image single CNCs and is expected to generate information on the distribution of the CNCs in the CNC-PP composite. Among numerous other applications, the mapping technique has been used to investigate the distribution of cellulose and lignin in the cell walls of woody tissues.[16,17]

EXPERIMENTAL

The four samples analyzed by Raman techniques (Fourier transform (FT) Raman and confocal micro-Raman) included a PP control and three cellulose/PP composites as listed in Table I. The methods used in their preparation were as follows.

Cellulose Nanocrystal Preparation. CNC was prepared by sulfuric acid hydrolysis of wood pulp using 64% sulfuric acid (acid : cellulose = 8 : 1 (v : w)) by a procedure similar to that of Dong et al.[18] PP (Certene PHM-20) and maleic anhydride grafted polypropylene (MAPP) (Eastman Chemical; Epolene G-3015) were obtained commercially. Microcrystalline cellulose (MCC) labeled as Avicel 591f was obtained from FMC Biopolymer. This MCC contained carboxymethylcellulose as a dispersant.

The CTAB (cetyl trimethyl ammonium bromide) form of CNC was prepared by neutralizing an aliquot of CNC with solid sodium bicarbonate. A stoichiometric amount of CTAB was dissolved in a small amount of warm water (1/10 of CNC aliquot). (The CNC preparation typically produces CNC containing about 1wt. % sulfur (as surface sulfate esters); the

0003-7028/12/6607-0750$2.00/0

TABLE I. Samples analyzed by Raman mapping.

Sample ID	Description[a]
PP-CON	PP, control
AC_CNC-PP	Acetylated CNC:PP = 2:98
FRACT_CNC-PP	NanoF-MCC:MAPP:PP = 2:2:96
MAPP_CNC-PP	CNC:MAPP:PP = 2:2:96

[a] PP = Polypropylene; CNC = cellulose nanocrystal; MAPP = maleated polypropylene; nanoF-MCC = nano-crystalline fraction of microcrystalline cellulose.

amount of CTAB was calculated as a 1 : 1 molar stoichiometry.) The CTAB solution was added quickly to the stirred CNC aliquot. This suspension was centrifuged and the clear liquid decanted. The CNC was washed by suspending in water and centrifuging three times. A solvent exchange was performed on the CNCs by suspending them in a series of solvents three times each and centrifuging. The solvents used were 95% ethanol followed by acetone, diethyl ether, and then xylenes (Sigma-Aldrich, ≥98.5%).

CNC-PP Composite Preparation (MAPP_CNC-PP). In a round-bottom flask, 43 g of 4.65 wt. % CTAB-CNCs in xylenes were added to 150 mL of xylenes, 2 g of MAPP, and 30 mL of pyridine. These were refluxed under nitrogen with stirring for 16 hours. PP (96 g) was dissolved in 800 mL of xylenes at boiling. The CNC/MAPP reaction mixture was added to the dissolved polypropylene and mixed for 10 minutes. The composite was allowed to cool, transferred onto aluminum foil, and the xylenes allowed to evaporate (solution casting method). The composite was then placed in a vacuum oven at 125 °C overnight.

Acetylated CNC-PP Composite (AC_CNC-PP). Acetylated CNCs were prepared according to similar reaction procedures described above where acetic anhydride was substituted for MAPP. The preparation of the polypropylene composite followed the same protocol as above.

Fractionated MCC-PP Composite (FRACT_CNC-PP). Nanocrystalline cellulose particles were obtained by fractionating commercial MCC. MCC was repeatedly centrifuged, decanted, and diluted until the nanocrystalline fraction was obtained. This fraction was then compounded with PP and MAPP in a high-shear thermokinetic mixer at 5000 rpm and granulated.

PP (PP-CON). One hundred grams (100 g) PP was dissolved in 900 mL of boiling toluene. The solution was allowed to cool and the PP was transferred onto aluminum foil and the toluene allowed to evaporate. The PP was then placed in a vacuum oven at 125 °C overnight. The PP was dissolved and isolated in this manner in order for the treatment to be analogous to that used in the preparation of the composites.

Extrusion. The powder resulting from the solvent casting of samples PP-CON, AC_CNC-PP, and MAPP_CNC-PP and the compounded sample (FRACT_CNC-PP) were milled to ~ 20 meshes in a Wiley Mill. The materials were then extruded into filaments using a Laboratory Mixing Extruder (Dynisco) with a 3 mm die orifice. The temperature of the rotor and die was set to 185 °C and 175 °C, respectively. The rotor and uptake speeds were adjusted to give a 1 mm nominal fiber diameter.

Transmission Electron Microscopy. A Philips CM-100 transmission electron microscope (TEM) at 100 kV, spot 3, 200 μm condenser aperture, and 50 μm objective aperture was used. This instrument was calibrated using a replica grating. CNC particles were deposited on a TEM grid (400 mesh Formvar/carbon filmed grid prepared with blow discharge) by floating the grid on CNC suspension (~0.05 wt% concentrations) droplets for ~2 minutes then rinsing through 2% aqueous uranyl acetate stained and blotted dry.

Raman Analysis and Mapping. The FT-Raman spectra were obtained using a Bruker RFS-100 spectrometer (Bruker Optics Inc.) equipped with a 1 W, 1064 nm Nd : YAG diode-pumped laser. The PP and composite samples were directly analyzed whereas CNC and acetylated CNC were sampled in the "aluminum well" sampling accessory. The laser power used for sample excitation was 600 mW, and 1024 scans were accumulated with the use of a double-sided forward–backward scanning mode. The samples were analyzed in 180° geometry. Bruker's OPUS software program was used to find peak positions and process the spectral data.

For Raman mapping, sample cross-sections, 30 μm thick, of extruded fibers were analyzed using a 633 nm based Raman microprobe spectrometer, LabRam HR 800 (Horiba Jobin Yvon). This spectrometer is equipped with a confocal microscope (Olympus BX40), a piezoelectric x, y stage, and a charge-coupled device (CCD) detector. The instrument provides ultra-high spectroscopic resolution and unique polarized 633 nm laser (20 mW) excitation. Spectra of samples PP-CON, AC_CNC-PP, FRACT_CNC-PP, and MAPP_CNC-PP from various sample regions were obtained by using the serial (raster) mapping technique. Each sample was placed on an automated piezoelectric x, y mapping stage and Raman spectra were obtained at different points on the surface by moving it equivalently under the microscopic objective. For mapping in the x, y plane at a chosen stepping resolution (2, 1, or 0.5 μm), the specimen was moved in the two spatial dimensions (x and y) and a spectrum was recorded at each (x, y) position. Lower stepping resolution was used to increase the speed of mapping. For a region of fixed size, the number of spectra acquired is proportional to $1/n^2$ where n is the step resolution. An Olympus 100× MPlan metallurgical objective, NA 0.90, was used for the Raman studies. The component-specific Raman image of a sample was constructed by plotting the area intensity of the selected band as a function of position. Raman images for both CNC and PP distributions were generated based on bands in the spectral region 800–1650 cm^{-1}. LabSpec 4.02 software was used to perform spectrometer operations, obtain Raman spectra, process the collected data, and generate Raman images. Additional details of the mapping process are similar to those reported earlier in Ref. 16.

For plotting purposes, Raman data were converted to ASCII format and then imported to Excel (Microsoft Corporation). The spectra were not smoothed and some were corrected for background contributions.

Tensile and Modulus Tests. The tensile testing of fiber samples was performed at 23 °C and 50% relative humidity using an MTS Insight testing system with a 100 N load cell. Fibers were clamped pneumatically using steel-toothed clamp faces. A one-inch gauge length was used, and the tests were performed with a crosshead speed of 1 inch per minute (strain rate of 1 min^{-1}). Samples were tested to failure, and the tensile stress was taken as the maximum stress level. The modulus was determined by fitting the data to a hyperbolic tangent curve and taking the slope of the fitted curve at the initial strain. At least 10 specimens were tested for each sample.

RESULTS AND DISCUSSION

The TEM micrograph of CNCs is shown in Fig. 1. The small width distribution and the high aspect ratio of the CNCs can be observed.

Raman Analysis. Previously, Raman spectroscopy has been used to analyze both PP and celluloses but not their composites.[20–25] In the case of PP, the method was used to estimate the crystallinity of isotactic polypropylene[20] and to study its polymorphs.[21] Similarly, for cellulose, a few of the applications were in the areas of molecular structure,[22] crystallinity,[23] and polymorphy.[24]

Fourier transform Raman spectra of PP, MAPP modified fractionated MCC, and acetylated CNCs, in the spectral region from 850 to 1550 cm^{-1}, are shown in Fig. 2. Band positions of acetylated CNCs and PP are listed in Table II. The Raman frequencies in Table II corresponded well with the values reported in the literature for cellulose, cellulose acetate, and PP.[20–28] Based on this information, along with the spectra of acetylated CNCs and PP (Figs. 2c and 2a, respectively) the bands of cellulose and PP were easily discerned in the spectrum of 50/50 MCC/MAPP composite (Fig. 2b). In Fig. 2c, two of the cellulose bands are identified at 1098 and 1120 cm^{-1} while numerous peaks in Fig. 2a and Fig. 2b are due to PP. Both these bands arise from the C–O–C stretching modes in cellulose.[25] In the FT-Raman spectra of CNCs, acetylated CNCs, and MCC most Raman peaks were present at similar wavenumber positions. FT-Raman spectra of acetylated and control CNCs are compared in Fig. 3. The hydroxyl groups of cellulose were esterified with acetic anhydride and could produce a variety of acetylated CNCs with properties that depend on the degree of acetylation. Compared to the cellulose spectrum (Fig. 3), in the spectrum of acetylated CNCs new bands appeared at 1740 and 2938 cm^{-1} (C=O and acetyl C–H stretches, respectively), which indicated that the cellulose hydroxyl groups have been acetylated. Additionally, because upon acetylation the intensity of the 380 cm^{-1} band did not change at all, it was taken as evidence for the acetylation being limited to the surfaces of the CNCs. Had acetylation taken place in the bulk, the band intensity at 380 cm^{-1} would have declined very significantly[26] (the 380 cm^{-1} band declined drastically when the degree of acetylation was 1.07).[26] In this context, no reduction in band intensity also implied no change in cellulose crystallinity,[23] which is what one would expect if the acetylation reaction was indeed limited to the crystalline surfaces.

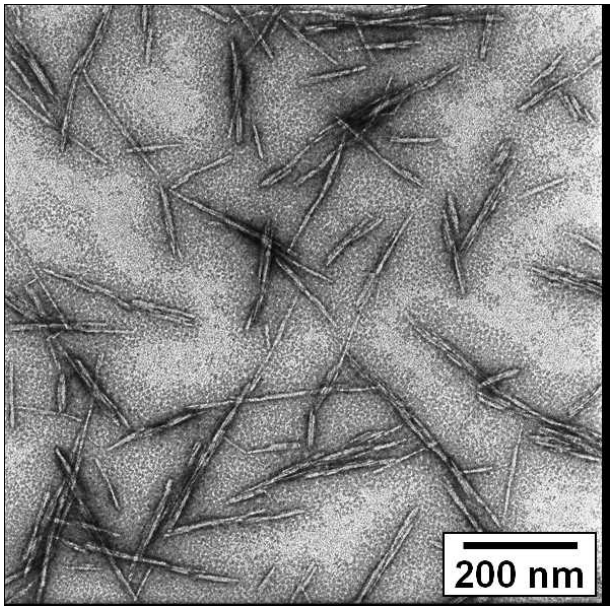

FIG. 1. Transmission electron image of cellulose nanocrystals derived from wood.[19]

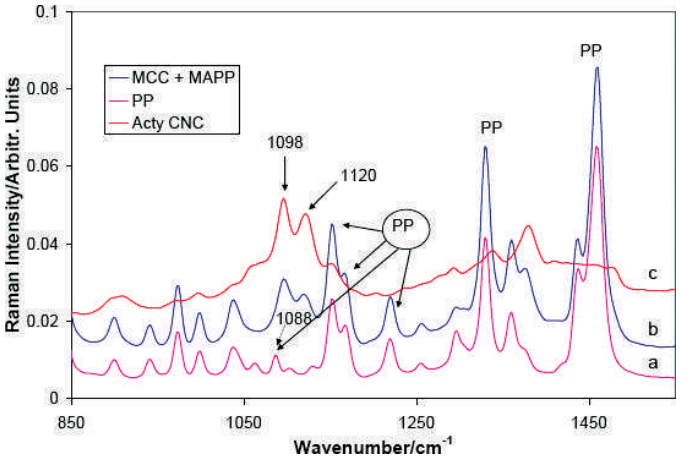

FIG. 2. FT-Raman spectra of (*a*) PP, (*b*) 50/50 fractionated MCC/MAPP, and (*c*) acetylated CNC in the region 850–1550 cm^{-1}. Compared to PP, cellulose signals are weaker, although contributions at 1098 and 1120 cm^{-1} due to the latter could be easily detected in the MCC/MAPP composite spectrum.

In the FT-Raman spectra of PP containing the nanocelluloses, the cellulose bands could not be detected due to the low concentration of nanocellulose and, compared to PP, significantly lower Raman scattering cross-section. One set of such spectra, in the region 250 to 1650 cm^{-1}, is shown in Fig. 4. The spectra are superimposed for ease of comparison and were normalized on the 809 cm^{-1} band of PP. No band due to crystalline cellulose at 1098 cm^{-1} can be detected. Crystalline cellulose scatters moderately at this wavenumber (Fig. 2c). In Fig. 4, the weak bands present at 1088, 1104, and 1130 cm^{-1} belong to PP. Nevertheless, concerned that CNC was not dispersed homogenously in the composites, it was decided to study its distribution by Raman microscopy where spatially resolved spectra from microscopic domains are obtained. A sample of PP was also included in such an investigation to obtain spatially resolved information on PP fibers.

Polypropylene Distribution in the Control Sample. A map of PP distribution in sample PP-CON was generated using the 1413–1500 cm^{-1} region Raman intensity (peak position 1460 cm^{-1}) (Fig. 5a). The 1460 cm^{-1} region bands of PP are due to the methyl group deformations.[20] The image intensity of PP in the cross-section surface was found to be non-uniform. This is likely due to variations in the physical state (crystalline versus amorphous) and/or crystallite orientation. Effects of such factors on PP Raman spectrum have been studied previously.[20,21] Martin et al.[21] reported that the band intensities between the Raman spectra of α-spherulite and β-spherulite crystalline forms of PP differed. Additionally, their work reported that the polarized Raman spectra of the β-spherulite polypropylene revealed the existence of crystalline orientation anisotropy within the crystalline phase. To visualize the contribution of the weak PP bands (1088 1104, and 1130 cm^{-1}) that were present in the cellulose imaging region, a map

TABLE II. Raman band positions (cm^{-1}), 250–1650 cm^{-1} region, in the spectra of acetylated CNCs and polypropylene.[a]

Acetylated CNCs	Assignments[b]	Polypropylene (PP)	Assignments[d]
331 sh	Heavy atom bending[c]	282 vw	Not assigned
348 w	Some heavy atom stretching	320 m	~CH_3 wagging, CH_3 bending
381 m	Some heavy atom stretching	399 s	C–C bending, C–CH_3 bending
437 m	Some heavy atom stretching	457 m	C–C bending, C–CH_3 bending
459 m	Some heavy atom (CC and CO) stretching	528 m	C–C bending, ~CH_3 wagging, C–CH_3 bending
492 w	Some heavy atom (CC and CO) stretching	809 s	Coupled C—H deformation C–C stretching
520 m	Some heavy atom (CC and CO) stretching	842 s	CH_2 rocking, CH_3 rocking, C–C stretching
566 w	Not assigned	900 w	Coupled C–H deformation C–C stretching
607 w	Acetyl group	941 w	Coupled C–H deformation, C–C stretching
639 w	Acetyl group	973 m	CH_3 rocking, CH_2 rocking, C–C stretch
751 w	Not assigned	999 m	C—C stretching, –CH_3 rocking, CH_2 rocking
898 m	HCC and HCO bending at C-6	1038 m	C–C stretching, ~CH_3 wagging
909 m	HCC and HCO bending at C-6	1063 w	C–C stretching
971 w	Not assigned	1088 w	Coupled C–H deformation, C–C stretching
997 w	Stretching (CC and CO)	1104 vw	C–C bending, CH_3 rocking
1037 sh	Stretching (CC and CO)	1130 vw	C–C stretching, C–C bending, CH_3 rocking
1063 sh	Stretching (CC and CO)	1152 s	–CH_3 wagging
1073 sh	Stretching (CC and CO)	1167 m	~CH_3 wagging, C–C stretching
1098 s	Stretching (CC and CO)	1219 m	–CH wagging
1120 s	Stretching (CC and CO)	1255 w	–CH wagging
1152 m	Heavy atom stretching plus HCC and HCO bending	1296 m	–CH_2 twisting
1294 m	HCC and HCO bending	1330 s	–CH_2 wagging
1339 m	HCC, HCO, and HOC bending	1360 m	–CH bending
1380 m	HCC, HCO, and HOC bending	1437 m	–CH_2 bending
1409 sh	HCC, HCO, and HOC bending	1460 vs	–CH_3 bending
1456 sh	HCH and HOC bending	—	—
1478 m	HCH and HOC bending	—	—

[a] Note: Band intensities are relative to other bands in the spectrum: vs is very strong; s is strong; m is medium; w is weak; vw is very weak; sh is shoulder.
[b] Assignments from Refs. 25 and 26.
[c] Heavy atoms mean CCC, COC, OCC, and OCO modes.
[d] Assignments from Refs. 27 and 28.

was generated using these bands (Fig. 6). The Raman image suggested that in various PP-CON sample regions the concentration of PP as measured by the area integration of the 1088, 1104, and 1130 cm^{-1} bands was close to zero. This is further supported by the presence of very low intensity, more or less continuous, dark blue regions in Figs. 5b to 5d which arise, in the absence of CNCs, from the integration of the weak PP bands (1088, 1104, and 1130 cm^{-1}) . The latter implies that the existence of such nearby PP bands poses no problem for studying the distribution of CNCs.

CNC Distribution in the PP Composites. Cellulose bands at 1098 and 1120 cm^{-1} (region 1079–1140 cm^{-1}) were used to visualize the spatial distribution of CNCs in the samples of the three composites [Figs. 5b–5d]. These images represent some of the many regions that were investigated in each sample. Spectra from the selected points in the cellulose-rich regions in the images contained strong features of cellulose. Although in the cellulose imaging region 1079–1140 cm^{-1}, weak PP features at 1088, 1104, and 1130 cm^{-1} exist, their contributions to the images were found to be negligible based on the 1079–1140 cm^{-1} region identical Raman imaging in the control sample PP-CON (Fig. 6). Moreover, for the purposes of investigating the cellulose distribution, the CNCs were assumed to be randomly oriented in the samples.

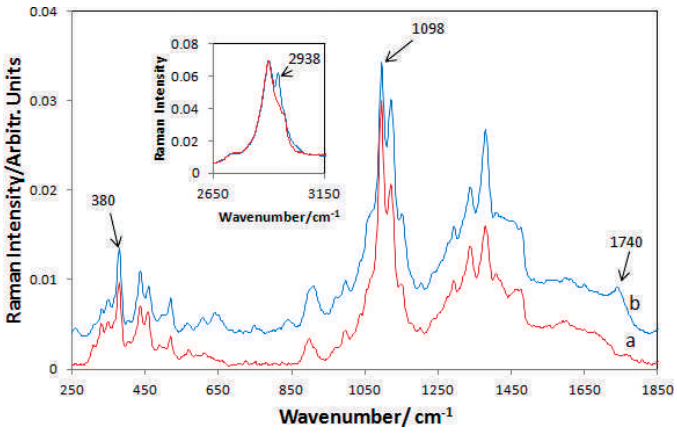

FIG. 3. FT-Raman spectra of (*a*) CNCs and (*b*) acetylated CNCs. The inset shows the C–H stretch region.

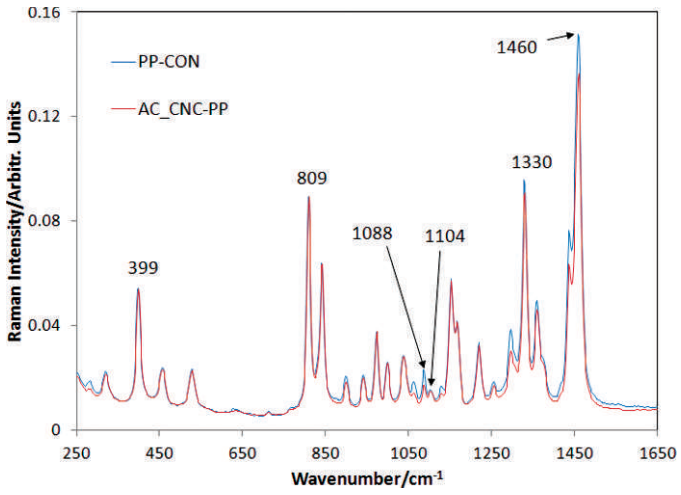

FIG. 4. FT-Raman spectra of PP (PP-CON) and acetylated CNC : PP (AC_CNC-PP) shown in the region 250–1650 cm^{-1}.

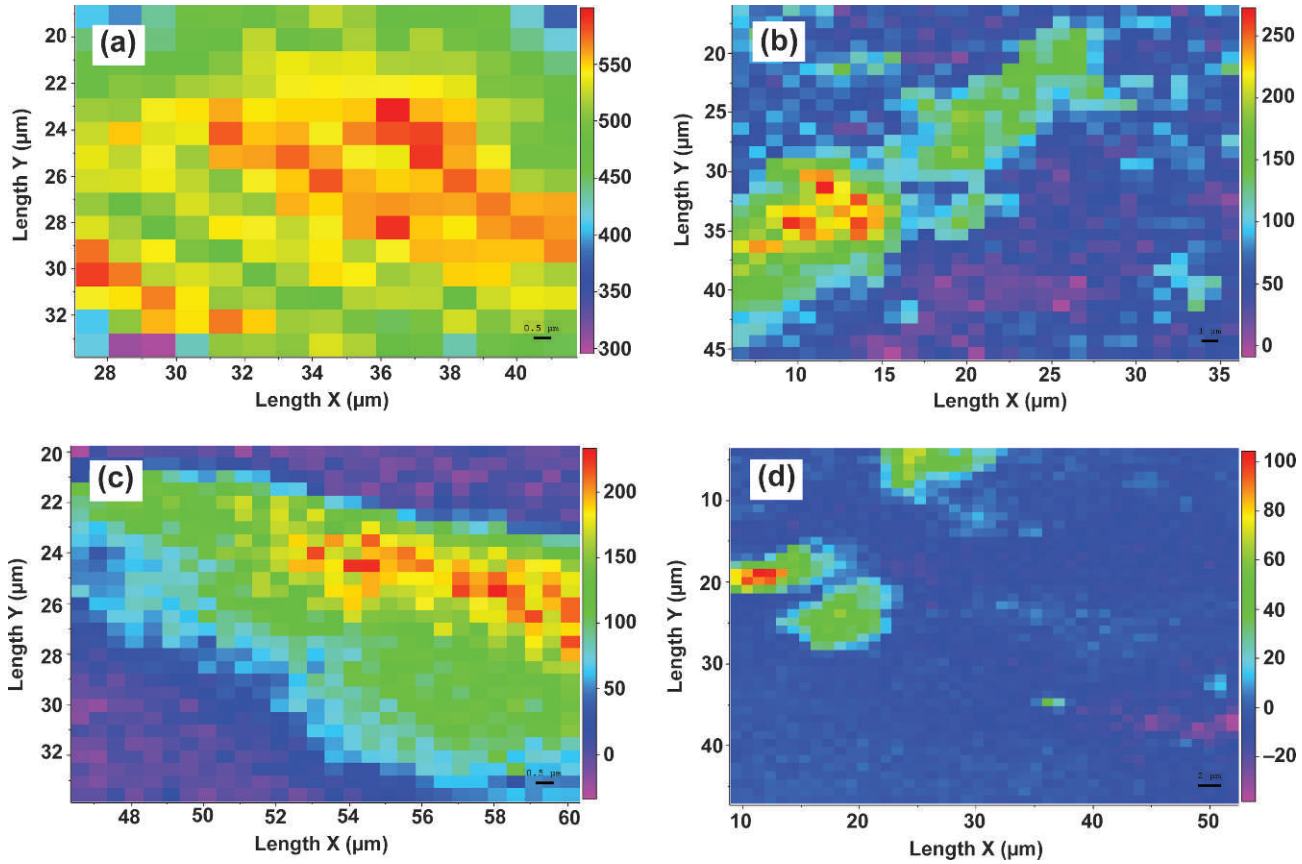

FIG. 5. Raman images (false color) of spatial distributions of composite components: (**a**) PP in sample PP-CON, (**b**) CNCs in sample AC_CNC-PP, (**c**) CNCs in sample FRACT_CNC-PP, and (**d**) CNCs in sample MAPP_CNC-PP. Note the different scale bar values in different images (a = 0.5 μm, b = 1 μm, c = 0.5 μm, d = 2 μm). The intensity scale for each Raman map appears on the right of the image. High, medium, and very low component concentrations are indicated as red, green, and blue regions, respectively. Some locations show negative values and arise from the manner in which intensities were calculated for the images.

For the composites, when the Raman images based on the PP and cellulose bands were compared, it became clear that they were almost complementary to each other. PP images of the composites are not shown in this paper. However, in regions where cellulose intensity is close to zero in Fig. 5, PP intensity was high. In other words, in locations where PP was strong, cellulose was weak or absent, and vice versa. Therefore, a phase dominant structure clearly existed in the sample regions. The CNC-rich regions were present as big- and small-aggregates (AC_CNC-PP or FRACT_CNC-PP and MAPP_CNC-PP, respectively) and the PP-abundant regions were present as continuous phases. A summary of the Raman mapping study and tensile tests are provided in Table III.

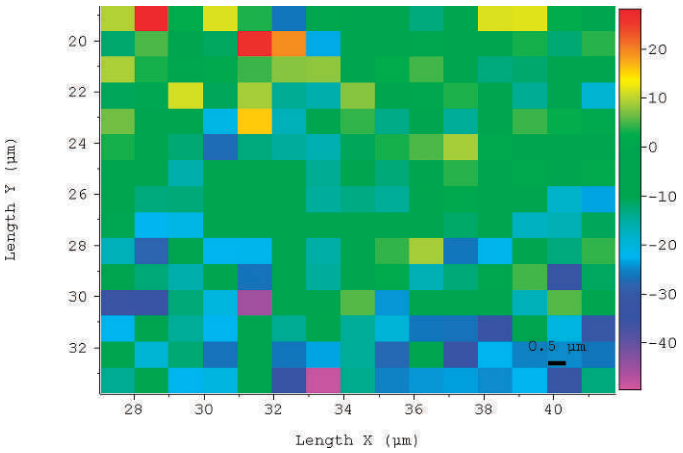

FIG. 6. Raman image of the PP-CON sample generated using the cellulose imaging region (1079–1140 cm^{-1}). The image has minimal intensity (close to zero) in most mapped regions, indicating that the weak PP bands present at 1088, 1104, and 1130 cm^{-1} do not pose a difficulty in studying cellulose distribution.

Table III lists various parameters (column 1) used in the context of the Raman mapping study. For instance, the number of scans indicates how many different regions of a sample were analyzed and the average domain size is the average dimension of cellulose (the dispersed phase) in the blend. Comparing the percentage of scans that showed cellulose for the three composite samples (Table III, row 4), for sample FRACT_CNC-PP, just 15% showed detectable cellulose, which was more than four times lower than found in samples AC_CNC-PP and MAPP_CNC-PP. This is due to the presence of larger size aggregates of CNCs in this sample (Table III, row 6). Differences between the average scan sizes of the samples did not seem to be important because compared to FRACT_CNC-PP both the lower (in AC_CNC-PP) and higher (in MAPP_CNC-PP) scan sizes had higher probability of detecting CNCs (Table III, row 5).

A dispersion index (DI) can be determined that is analogous to the compatibility number in polymer blends, which indicates mixing at the molecular level. In the case of nanocrystals,

TABLE III. Summary of Raman mapping study and tensile and modulus data.

Parameter	Fiber ID			
	PP-CON	AC_CNC-PP	FRACT_CNC-PP	MAPP_CNC-PP
Number of scans	15	11	20	15
Number of scans that showed cellulose	NA	8	3	12
% of scans with cellulose	NA	72	15	80
Average area of scans, μm^2	22 × 23	21 × 29	32 × 39	36 × 38
Cellulose dispersion; average domain size, μm^2	NA	Aggregated; 78	Aggregated; 120	Better dispersed; 16
Dispersion index, DI	NA	0.013	0.008	0.063
Tensile stress, MPa	34.0 ± 1.8[a]	—	35.4 ± 2.4	37.5 ± 2.2
Modulus, MPa	990.0 ± 78.2[a]	—	814.1 ± 106.4	1156.6 ± 133.9

[a] Standard deviation.

dimensions are considerably larger than polymer molecules, but this is still analogous to many heterogeneous systems that can be considered as compatible though they show a large degree of phase separation and two distinct glass transitions. Thus the compatibility or homogeneity of a polymer blend is related to both the experimental probe size and the domain size of the phase.[29] A dispersion index is here defined as DI = Experimental probe size/Domain size. When DI = ∞ the blend is well dispersed, when DI = 1, the blend is moderately well dispersed, and when DI = 0 the blend is poorly dispersed. Taking the probe size as one micron for the Raman microprobe, the values for dispersion number were calculated and are reported in Table III. Clearly, none of the composite blends came close to being even moderately well dispersed although for the MAPP_CNC-PP blend the dispersion number was significantly higher than for AC_CNC-PP and FRACT_CNC-PP. This was further supported by the fact that, in the Raman maps (Fig. 5), a clear transition interface between the PP-abundant and CNC-abundant regions was observed and was a reflection of the fact that they are two discrete phases.

Tensile and Modulus Tests. Tensile and modulus tests (Table III) of fiber samples with CNCs indicated up to 10 to 17% improvement (e.g., MAPP_CNC-PP) compared to PP alone and, based on the t-significance testing ($P = 0.05$), the mean test values of the MAPP_CNC-PP and PP were different. Further statistically meaningful improvements in the mechanical properties of the composites are expected to result from an improved CNC-PP interface and better dispersion. Moreover, the mean mechanical test values of MAPP_CNC-PP were higher compared to FRACT_CNC-PP (Table III). Based on the Raman images, the former nano-composite also had better dispersion of CNCs in the PP matrix (Fig. 5d). This suggests that better dispersion of CNCs is likely to lead to a stronger CNC-PP composite.

CONCLUSIONS

Three different PP composites containing 2% CNC were prepared and characterized using Raman mapping and tensile test methods. Compared to PP, gains in the mechanical properties of the extruded composite fibers were found to be statistically significant. A Raman mapping investigation to characterize the composites in a spatially resolved manner performed at the microscopic level revealed that the CNC was poorly dispersed in the PP, although adding MAPP improved the situation slightly. Improved methods of CNC-PP composite preparation are needed, but this investigation demonstrated the usefulness of the Raman mapping technique for evaluating dispersion at the microscopic level.

ACKNOWLEDGMENT

We thank Robert Moon at Forest Products Laboratory, Madison, WI for providing the TEM micrograph of the CNCs.

1. M.J. John, S. Thomas. "Biofibres and Biocomposites". Carbohydr. Polym. 2008. 71(3): 343-364.
2. A.K. Mohanty, M. Misra, L.T. Drzal. "Sustainable Bio-Composites from Renewable Resources: Opportunities and Challenges in the Green Materials World". J. Polym. Environ. 2002. 10: 19-26.
3. A.A. Klyosov. Wood-Plastic Composites. Hoboken, NJ: John Wiley & Sons, 2007. Pp. 698.
4. R.M. Rowell, A.R. Sanadi, D.F. Caulfield, R.E. Jacobson. "Utilization of Natural Fibers in Plastic Composites: Problems and Opportunities". In: A.L. Leao, F.X. Carvalho, E. Frollini, editors. Lignocellulosic Plastic Composites. Sao Paulo, Brazil: USP/UNESP, 1997. Pp. 23-51.
5. C.M. Clemons. "Wood-Plastic Composites in the United States: The Interfacing of Two Industries". Forest Prod. J. 2002. 52(6): 10-18.
6. S.J. Eichhorn, A. Dufresne, M. Aranguren, N.E. Marcovich, J.R. Capadona, S.J. Rowan, C. Weder, W. Thielemans, M. Roman, S. Renneckar, W. Gindl, S. Veigel, J. Keckes, H. Yano, K. Abe, M. Nogi, E.A.N. Nakagaito, A. Mangalam, J. Simonsen, A.S. Benight, A. Bismarck, L.A. Berglund, T. Peijs. "Review: current international research into cellulose nanofibres and nanocomposites". J. Mater. Sci. 2010. 45(1): 1-33.
7. V. Favier, H. Chanzy, J.Y. Cavaille. "Polymer Nanocomposites Reinforced by Cellulose Whiskers". Macromol. 1995. 28(18): 6365-6367.
8. A. Šturcová, G.R. Davies, S.J. Eichhorn. "Elastic Modulus and Stress-Transfer Properties of Tunicate Cellulose Whiskers". Biomacromolecules. 2005. 6(2): 1055-1061.
9. Y. Kim, R. Jung, H.S. Kim, H.J. Jin. "Transparent Nanocomposites Prepared by Incorporating Microbial Nanofibrils into Poly(L-Lactic Acid)". Curr. Appl. Phys. 2009. 9(1): S69-S71.
10. H. Yano, J. Sugiyama, A.N. Nakagaito, M. Nogi, T. Matsuura, M. Hikita, K. Handa. "Optically Transparent Composites Reinforced with Networks of Bacterial Nanofibers". Adv. Mater. 2005. 17(2): 153-155.
11. S. Beck-Candanedo, M. Roman, D.G. Gray. "Effect of Reaction Conditions on the Properties and Behavior of Wood Cellulose Nanocrystal Suspensions". Biomacromolecules. 2005. 6(2): 1048-1054.
12. J.F. Kennedy, G.O. Phillips, P.A. Williams. Cellulose Sources and Exploitation: Industrial Utilization, Biotechnology, and Physico-Chemical Properties. New York, NY: Ellis Horwood, Ltd., 1990.
13. K. Tashiro, M. Kobayashi. "Theoretical Evaluation of Three-Dimensional Elastic Constants of Native and Regenerated Celluloses: Role of Hydrogen Bonds". Polymer. 1991. 32: 1516-1526.
14. T. Nishino, K. Takano, K.J. Nakamae. "Elastic Modulus of the Crystalline Regions of Cellulose Polymorphs". J. Polym. Sci., Part B: Polym. Phys. 1995. 33(11): 1647-1651.
15. G. Turrell, J. Corset, editors. Raman Microscopy—Developments and Applications. San Diego, CA: Academic Press, 1996.
16. U.P. Agarwal. "Raman Imaging to Investigate Ultrastructure and Composition of Plant Cell Walls: Distribution of Lignin and Cellulose in Black Spruce Wood (*Picea mariana*)". Planta. 2006. 224(5): 1141-1153.
17. N. Gierlinger, M. Schwanninger. "Chemical Imaging of Poplar Wood Cell Walls by Confocal Raman Microscopy". Plant Physiol. 2006. 140: 1246-1254.

18. X.M. Dong, T. Kimura, J.-F. Rovol, D.G. Gray. “Effects of Ionic Strength on the Phase Separation of Suspensions of Cellulose Crystallites”. Langmuir. 1996. 12: 2076-2082.
19. R.J. Moon, A. Martini, J. Nairn, J. Simonsen, J. Youngblood. “Cellulose Nanomaterials Review: Structure, Properties and Nanocomposites”. Chem. Soc. Rev. 2011. 40: 3941-3994.
20. A.S. Nielsen, D.N. Batchelder, R. Pyrz. “Estimation of Crystallinity of Isotactic Polypropylene Using Raman Spectroscopy”. Polymer. 2002. 43(9): 2671-2676.
21. J. Martin, P. Bourson, A. Dahoun, J.M. Hiver. “The β-Spherulite Morphology of Isotactic Polypropylene Investigated by Raman Spectroscopy”. J. Appl. Spectrosc. 2009. 63(12): 1377-1381.
22. J.H. Wiley, R.H. Atalla. “Raman Spectra of Celluloses”. In: R.H. Atalla, editor. Solid State Characterization of Cellulose. Washington, D.C.: American Chemical Society, 1987. ACS Symposium Series 340, Pp. 151-168.
23. U.P. Agarwal, R.S. Reiner, S.A. Ralph. “Cellulose I Crystallinity Determination Using FT-Raman Spectroscopy: Univariate and Multivariate Methods”. Cellulose. 2010. 17: 721.
24. R.H. Atalla. “Raman Spectral studies of Polymorphy in Cellulose. Part I: Celluloses I and II”. Appl. Polym. Symp. 1976. 28: 659-669.
25. J.H. Wiley, R.H. Atalla. “Band Assignments in the Raman-Spectra of Celluloses”. Carbohydr. Res. 1987. 160: 113-129.
26. K. Zhang, A. Feldner, S. Fischer. “FT Raman Spectroscopic Investigation of Cellulose Acetate”. Cellulose. 2011. 18: 995-1003.
27. M.P. McDonald, I.M. Ward. “The Assignment of the Infra-Red Absorption Bands and the Measurement of Tacticity in Polypropylene”. Polymer. 1961. 2: 341-355.
28. H. Tadakoro, M. Kobayashi, M. Ukita, K. Yasufuku, S. Murahashi, T. Torii. “Normal Vibrations of the Polymer Molecules of Helical Conformation. V. Isotactic Polypropylene and Its Deuteroderivatives”. J. Chem. Phys. 1965. 42: 1432-1449.
29. D.S. Kaplan. “Structure–Property Relationships in Copolymers to Composites: Molecular Interpretation of the Glass Transition Phenomenon”. J. Appl. Polym. Sci. 1976. 20(10): 2615-2629.